Available online at www.sciencedirect.com
ScienceDirect
Tetrahedron 64 (2008) 1743–1752
Tetrahedron
www.elsevier.com/locate/tet

# Accurate conformation analysis in solution: NMR and DFT/PCM study of the *S*-3-(1-naphthoyl)-4-isopropyl-2,2-dimethyloxazolidin-5-one in $CDCl_3$

Mathieu Branca [a], Valérie Alezra [a], Cyrille Kouklovsky [a], Pierre Archirel [b,*]

[a] *Laboratoire des Procédés et Substances Naturelles, ICMMO, UMR 8182, Bât. 410, Université Paris-Sud, F-91405 Orsay Cédex, France*
[b] *Laboratoire de Chimie-Physique, UMR 8000, Bât. 349, Université Paris-Sud, F-91405 Orsay Cédex, France*

Received 28 September 2007; received in revised form 23 November 2007; accepted 2 December 2007
Available online 9 January 2008

**Abstract**

The title molecule has been synthesised and the low temperature NMR spectrum recorded in $CDCl_3$. The spectrum shows that four conformers lie within 0.08 eV at 210 K. We show that an accurate conformation analysis can be obtained with a full and consistent use of the DFT (B3LYP) and PCM methods. If the polarised Stuttgart–Dresden basis and a PCM cavity with individual spheres on the hydrogen atoms are used, if the thermal and PCM non-electrostatic contributions are taken into account, and if a demanding convergence is achieved, then the rms error on the energy differences amounts to 0.002 eV. The 6-31+$g(d)$ basis is larger and yields a larger rms error: 0.006 eV.


*Keywords:* Aromatic amide; Conformation analysis; PCM method; Stuttgart–Dresden gaussian basis

## 1. Introduction

DFT (Density Functional Theory) and PCM (Polarised Continuum Medium) methods are widely used in the literature for conformation analysis of molecules, but in a wide range of ways. Many authors perform geometry optimisations in the vacuum and single point PCM calculations for solvation effects,[1] most authors define their cavity within the *United Atoms* frame, including the hydrogens in spheres centered on the heavy atoms to which they are bound, but some authors also define the cavity with a unique sphere.[2,3] Most authors use the gaussian basis sets of the Pople family[4] but with large variations in the choice of diffuse and polarisation functions, and contraction scheme. Results are only in 'reasonable' agreement with experiments, so that the question remains whether or not quantum chemistry can accurately interpret organic chemistry in solution.

In the present work we systematically investigate the main parameters of the PCM method, applied to the conformation analysis of the title molecule oxazolidin-5-one, which is a rather large molecule (44 atoms) and displays four conformers in less than 0.1 eV. We show that an excellent agreement with measurements can be obtained with the DFT and PCM methods, if the dielectric cavity and the gaussian basis set are carefully chosen, and if a demanding convergence of the DFT calculation is achieved.

Most tertiary aromatic amides **1** (Fig. 1) are not planar, and even moderate steric hindrance forces a dihedral angle of 90° on the Ar–CO bond.[5] Depending on substitution pattern (such as

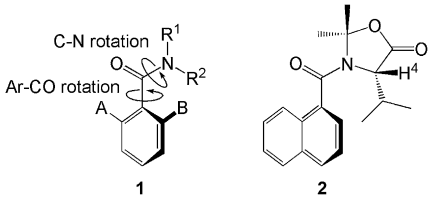


1 2

Figure 1. Tertiary amides (**1**) and the choice of the present work (**2**).

* Corresponding author. Fax: +33 1 69 15 61 88.
*E-mail address:* pierre.archirel@lcp.u-psud.fr (P. Archirel).

0040-4020/$ - see front matter © 2007 Elsevier Ltd. All rights reserved.
doi:10.1016/j.tet.2007.12.001

A≠B), the two perpendicular conformers about the Ar–CO bond are enantiomeric, and with a sufficiently slow rate of rotation about this bond, the conformers can be atropisomeric.[6–8] For simple amides **1** bearing achiral substituents A, B, $R^1$ and $R^2$, the rate of rotation about the Ar–CO bond is also the rate of enantiomerisation. When the amide bears chiral substituents A, B, $R^1$ or $R^2$, the conformers about Ar–CO are diastereoisomeric and at equilibrium they are not necessary equally populated. These properties have been elegantly exploited by Clayden[9–13] and other groups[14–17] in asymmetric synthesis.

For amides bearing chiral substituents A, B, $R^1$ or $R^2$ four conformers can be observed by $^1$H NMR at low temperature. These conformers interconvert by rotation about their Ar–CO (named *M*/*P* conformers) and C–N bond (named cis/trans conformers). The cis/trans conformers can be assigned by using the following property: signals of N-substituents cis to O are shifted downfield relative to those of N-substituents cis to the aromatic ring.[6] But there is no empirical means to assign the *M*/*P* conformers.

We are currently interested in oxazolidin-5-one **2** (Fig. 1), which actually displays four conformers in $^1$H NMR at low temperature. Hereafter the four conformers will be called *a* (*P* cis conformer), *b* (*M* cis conformer), *c* (*P* trans conformer) and *d* (*M* trans conformer). The four conformers are shown in Figure 2.

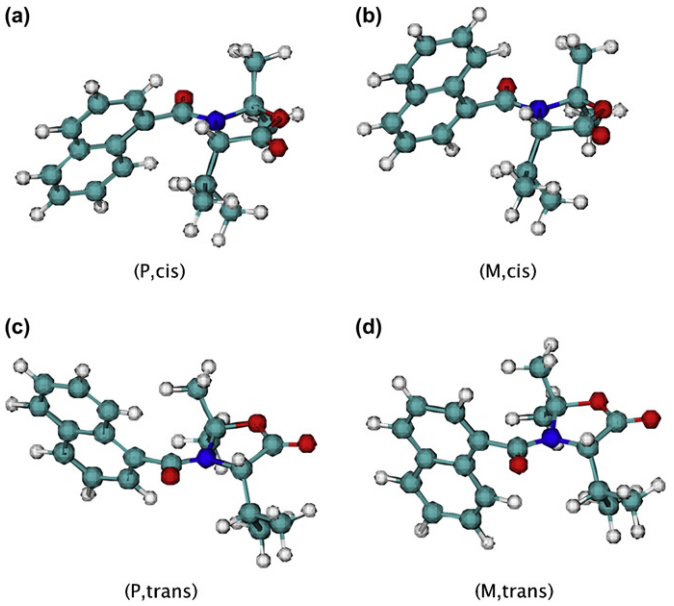


Figure 2. *S*-3-(1-Naphthoyl)-4-isopropyl-2,2-dimethyloxazolidin-5-one: the four conformers.

## 2. Results and discussion

### 2.1. Computational method

In the PCM method[18–20] the solute is imbedded in a cavity of a continuum medium fully characterised by its dielectric constant. This cavity is currently obtained through fusing spheres centered on nuclei and then *tesselised* with the help of little planar *tesseras*.[21] The radii of the spheres are essential parameters of the method, for which several choices can be made. In this work we use the van der Waals radii of the atoms, which have been evaluated in the frame of the *Universal Force Field* (UFF).[22] In all cases the cavity is enlarged with additional small spheres, which gives a smoother cavity surface and eliminates the dielectric from regions where the solvent is unlikely to penetrate.

We have investigated the following possibilities of the method:

1. Use of spheres centered on every atom, including H (true UFF cavity), or inclusion of H atoms in a (larger) sphere centered on the heavy atom (C, N) to which it is bound, as proposed by the *United Atom Topological Model* (UATM)[23] (UA–UFF cavity).
2. Inclusion of the PCM non-electrostatic terms (cavitation, dispersion, Pauli repulsion).
3. Convergence of the PCM energies towards the tesselation: we will use the values 0.1 and 0.2 Å$^2$ for the average value of the tessera surface.
4. Origin of the harmonic frequencies, calculated in the vacuum or in the cavity.
5. Convergence threshold of the DFT calculations.

All the quantum calculations have been performed with the B3LYP functional and basis sets of two origins: the 'Stuttgart–Dresden' (pSDD) core pseudopotentials and polarised basis set, and 'Pople' basis sets. Details are given in Section 5.1.

The ratio of $p_i$, abundance of conformer $i$ over $p_a$, abundance of conformer $a$ is related to the Gibbs free enthalpies $G$ and temperature $T$ through the Boltzmann formula.[24] Since $G$ and the Helmoltz free energy $F$ only differ through $PV$, and since $P\Delta V$ is usually fully negligible in solvation processes,[25] the formula may be written with free energies:

$$\frac{p_i}{p_a} = e^{-\frac{F_i - F_a}{kT}} \quad (1)$$

Conformation analysis can only be validated if the NMR spectrum is interpreted. For this reason we first present the calculation of the chemical shifts. The calculations have been done at the molecular geometries obtained with the UFF dielectric cavity and pSDD gaussian basis set, which will be justified in Section 2.4.

### 2.2. Chemical shifts

Part of the $^1$H NMR spectrum of compound **2** in $CDCl_3$ at 210 K (signals corresponding to $H^4$) is reproduced in Figure 3. This spectrum has been recorded at 210 K, which is the lowest temperature possible with liquid $CDCl_3$. The temperature uncertainty is 0.1 K. According to the argument of Clayden[6] the two largest peaks (on the right part of the spectrum) may be attributed to the cis conformers (*a* and *b*) and the two smallest peaks (left part of the spectrum) may be attributed to the trans conformers (*c* and *d*). Investigation of temperature effects has

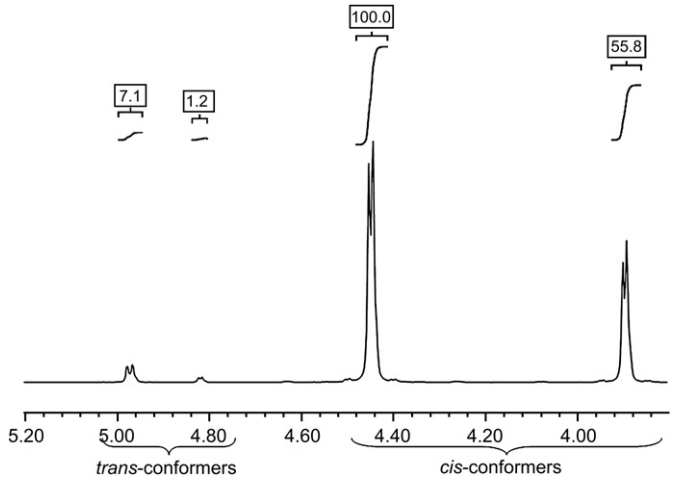


Figure 3. $H^4$ part of the NMR spectrum in $CDCl_3$ at 210 K.

shown that at about 290 K the coalescence of the *a* and *b* peaks on one side, and of the *c* and *d* peaks on the other side, is achieved. Complete coalescence of the four peaks has been obtained at about 320 K. Some exchange between the conformers at 210 K cannot be excluded, but we think that it is very slow. The chemical shifts are given relative to tetramethylsilane (TMS), with the usual sign convention:

$$\delta_{\mathrm{rel}} = \delta_{\mathrm{abs}}^{\mathrm{TMS}} - \delta_{\mathrm{abs}} \tag{2}$$

These chemical shifts have been calculated with the GIAO (Gauge Invariant Atomic Orbitals) method[26] and the 6-31$g(d,p)$ and 6-311+$g(2d,p)$ basis sets. We use two basis sets because it has been noted in the literature[27,28] that the calculated values of H chemical shifts are sensitive to the basis. The results for the four conformers, relative to the TMS value are given in Table 1 for the two basis sets. Absolute values for the TMS are 31.69 ppm (6-31$g(d,p)$ basis) and 31.81 ppm (6-311+$g(2d,p)$ basis). These results call for the following comments:

Table 1
Calculated and measured values of the NMR chemical shifts (in parts per million, relative to TMS) of $H^4$ in $CDCl_3$ for the four conformers and measured values of the peak surfaces

| | Origin | *c* (*P* trans) | *d* (*M* trans) | *a* (*P* cis) | *b* (*M* cis) | TMS |
|---|---|---|---|---|---|---|
| Shift | 6-31$g(d,p)$ | 4.88 | 4.72 | 4.38 | 3.99 | 0 |
| Shift | 6-311+$g(2d,p)$ | 5.07 | 4.92 | 4.57 | 4.14 | 0 |
| Shift | Exp. | 4.99 | 4.84 | 4.45 | 3.91 | 0 |
| Peak surface | Exp. | 7.1 | 1.2 | 100 | 55.8 | — |
| NBO charge | 6-311+$g(2d,p)$ | 0.251 | 0.249 | 0.241 | 0.243 | 0.226 |

1. Basis effects are present, but not larger than 0.2 ppm. This is exactly the error noted in the literature[27] for protons shifts in another class of molecules. Since the $c-d$ measured difference amounts to 0.15 ppm we must say that the interpretation of the NMR spectrum is not completely under control. Nevertheless the basis effect does not change the $c>d>a>b$ order of the chemical shifts, so that we may consider that this order yields a plausible interpretation of the spectrum.
2. Since this interpretation will be confirmed in the next sections by conformation analysis, we here admit it and deduce from peak surfaces the following order: $a<b<c<d$ of increasing energies.
3. The two highest peaks are attributed to the cis conformers (*a* and *b*) and the two smallest peaks to the trans conformers (*c* and *d*), so that our prediction, based on the analogy with Clayden compounds[6] is confirmed by the calculation.
4. The calculation also enables *M*/*P* discrimination. It can be seen that in both cis and trans case the *P* conformers (*a* and *c*) resonate at lower fields than the *M* conformers (*b* and *d*, respectively).
5. It is worth noting that the cis–trans identification can be predicted with the help of atomic charges, and that the *M*–*P* identification cannot. In Table 1 we give the NBO (Natural Bond Orbitals) charges[29] of hydrogen $H^4$ of the conformers and of the hydrogens of TMS. If we round up these charges to two figures, we get the following decreasing charges: $q_{\mathrm{trans}}$ (0.25)>$q_{\mathrm{cis}}$ (0.24)>$q_{\mathrm{TMS}}$ (0.23) in good correlation with the decreasing chemical shifts. Unfortunately the charges are too close to each other to help *M*–*P* discrimination as can be seen on the cis case.

The four conformers are present with the following peak surfaces: 100.0, 55.8±0.1, 7.1±0.3 and 1.2±0.1, where the errors have been deduced from a series of 10 independent integrations. The peak surfaces enable the evaluation of the conformer energetics with the help of formula 1: if the zero energy is set on conformer *a*, we get the following relative energies: *b*: 0.01056±0.00003 eV, *c*: 0.048±0.001 eV, *d*: 0.080±0.0015 eV. It can be seen that the four conformers lie within 0.080 eV, and that the uncertainty on the energy differences amount to 0.0015 eV, or less. The temperature uncertainty (0.1 K) has no significant consequences. Reproducing these energies is a challenge for quantum chemistry in solution.

### 2.3. Conformation analysis in the vacuum

In this section we consider the electronic energies $E_{\mathrm{el}}$ and the electronic and nuclear (vibrational and rotational) free energies $F_{\mathrm{tot}}$ of the conformers at $T$=210 K:

$$F_{\mathrm{tot}}(T) = E_{\mathrm{el}} + E_{\mathrm{vib}}(T) - TS_{\mathrm{vib}}(T) - TS_{\mathrm{rot}}(T) \tag{3}$$

where the nuclear thermal energies $E_{\mathrm{vib}}$ and entropies $S_{\mathrm{vib}}$ and $S_{\mathrm{rot}}$ are given by standard statistical thermodynamics of the harmonic oscillator and free rotator.[24] Since we are only interested in relative stabilities, we do not consider the translation and rotational thermal energies, and translational entropies neither, which exactly cancel out when energy differences are calculated.

The electronic energies, partial and total free energies are given in Table 2. All the vibration frequencies are real (not

Table 2
Absolute values (H) and relative values (eV) of electronic energies, partial (electronic and vibrational) and total (electronic, vibrational and rotational) free energies of the four conformers in vacuum

| | *a* | *b* | *c* | *d* |
|---|---|---|---|---|
| $E_{el}$ | −178.59706602 | −178.59640056 | −178.59410769 | −178.59214166 |
| $F_{elvib}$ | −178.238878 | −178.238155 | −178.235955 | −178.234313 |
| $F_{tot}$ | −178.250371 | −178.249616 | −178.247478 | −178.245801 |
| $E_{el}$ | 0 | 0.0181 | 0.0805 | 0.1340 |
| $F_{elvib}$ | 0 | 0.0197 | 0.0795 | 0.1242 |
| $F_{tot}$ | 0 | 0.0205 | 0.0787 | 0.1244 |
| $G_{rel}$ (exp.) | 0 | 0.0106 | 0.0480 | 0.0800 |

shown), this proves that the calculated structures are true minimas. Structural quantities, dihedral angles and dipole moments are given in Table 3. From Tables 2 and 3 the following comments can be made:

1. Conformer *a* is the most stable, the energy order is *a*<*b*<*c*<*d*. The four conformers lie within 0.13 eV.
2. It can be seen that the dipole moment of *c* and *d* is much larger (5.3 D) than that of *a* and *b* (3.4 D). A stabilisation of *c* and *d* can be expected in solution, therefore.
3. Vibrational and rotational contributions are small (but perceptible), and do not modify the stability order. Both nuclear contributions tend to destabilise *b* and to stabilise *c* and *d*, relative to *a*.
4. The values of the C(Me)NC(O)O dihedral angle show that in *a* and *b* the CO bond lies almost perfectly within the five-membered ring. We have also checked that in these cases the N atom displays three coplanar bonds. Both features are in agreement with simple ideas about maximum conjugation of the CO π bond and the lone pair of the ($sp^2$) N atom.
5. The values of the same dihedral angle show that in the *c* and *d* cases this conjugation is decreased. This feature goes along with an N atom, which is a little pyramidalised.
6. The values of the $C_{Ar}H_{Ar}C(O)N$ dihedral angle show that in every case the naphthyl group is twisted, as can be expected from steric hindrance of the isopropyl and dimethyl groups.

We emphasise that the four conformers have their four smallest frequencies between 30 and 60 $cm^{-1}$. The smallest frequency is that of the internal rotation of the naphthyl group about the $C_{Ar}C(O)$ bond.

Table 3
Characteristic dihedral angles (degrees) and dipole moment (Debye) of the different conformers in vacuum and in $CDCl_3$ in the UFF cavity

| Condition | Quantity | *a* | *b* | *c* | *d* |
|---|---|---|---|---|---|
| In vacuum | $C_{Ar}(H)C_{Ar}C(O)N$ | 62.29 | −117.42 | 58.23 | −110.43 |
| | C(Me)NC(O)O | 12.05 | 10.59 | −148.02 | −153.97 |
| | Dipole moment | 3.40 | 3.37 | 5.36 | 5.30 |
| In $CDCl_3$ | $C_{Ar}(H)C_{Ar}C(O)N$ | 64.80 | −115.95 | 61.98 | −106.54 |
| | C(Me)NC(O)O | 11.79 | 10.29 | −151.97 | −157.64 |
| | Dipole moment | 4.0276 | 4.0280 | 6.70 | 6.59 |

### 2.4. PCM energies

In this section we discuss the PCM energies of optimised structures, given by:

$$E_{pcm} = E_{pcm}^{el} + E_{pcm}^{non\ el} \quad (4)$$

where $E_{pcm}^{el}$ is the electrostatic energy of the molecule in the field of the polarised solvent and $E_{pcm}^{non\ el}$ gathers non-electrostatic contributions: cavitation,[30,23] dispersion[31,32] and Pauli repulsion[33] energies. As stated in the introduction we use the simple UA−UFF cavity, with spheres defined only on heavy atoms, and the more sophisticated UFF cavity, with spheres on every atom, including H. We use the dielectric constant of $CDCl_3$ (4.67[34]) and tesseras with an area value of 0.2 and 0.1 $Å^2$ in average. The basic radii of the spheres are the ones of the UFF model.[22]

#### 2.4.1. Uncertainty on the PCM energies

We first comment on the convergence of the calculations: we have found that geometry optimisations with residual forces smaller than $10^{-6}$ H $Å^{-1}$ are difficult as soon as cavities are used. This issue may be attributed to both the small frequencies of the molecule (close to 30 $cm^{-1}$) and the tesselation of the cavity surface, which yields ripples on the potential surface. We have ensured the smallest possible values of the residual forces, with the help of the Berny[35] and GDIIS (Generalised Direct Inversion in the Iterative Subspace) algorithms.[36] All the calculated structures are true minimas, with only real vibration frequencies (not shown).

The PCM energies and residual rms (root mean square) forces are given in Table 4, it can be seen that:

1. Full convergence (with residual forces smaller than $5.10^{-7}$ H $Å^{-1}$) has been obtained in many cases.
2. In a few cases the residual force is larger, but much smaller than $10^{-5}$ H $Å^{-1}$
3. In one case only (finest UFF calculation of the *b* conformer), the residual force reaches $10^{-5}$ H $Å^{-1}$.

We have evaluated the consequences of these residual forces with the help of a few fully converged calculations, assuming that all the conformers have the same convergence behaviour. The convergence route of these calculations is graphically summarised in Figure 4, where energy deviations from the final energy are given towards the corresponding values of the residual force, along the sequence of iterations. Figure 4 shows that for residual forces smaller than $5.10^{-6}$ H $Å^{-1}$ energy deviations are negligible (<0.0005 eV), and that for forces close to $10^{-5}$ H $Å^{-1}$ they hardly reach 0.001 eV. This suggests that for the finest UFF calculation of *b*, displaying the largest residual force, the uncertainty is very probably smaller than 0.001 eV and the *b*−*a* energy difference can be safely written as ±0.0005 eV.

Figure 4 also shows that energy uncertainty rapidly increases when the residual force increases, this shows that approximate convergence can make accuracy discussions irrelevant. Thanks

Table 4
Absolute (H) and relative (eV) PCM energies in $CDCl_3$, residual rms force (in H Å$^{-1}$) at the convergence, influence of the spheres on H atoms and of the PCM surface tesselation, average tessera area are in Å$^2$ and rms errors in eV

| PCM cavity+average tesserae area | | *a* | *b* | *c* | *d* | rms error |
|---|---|---|---|---|---|---|
| UA−UFF 0.2 | $E_{abs}$ | −178.592295 | −178.591177 | −178.591356 | −178.589709 | |
| | rms force | 0.000000 | 0.000001 | 0.000005 | 0.000001 | |
| | $E_{rel}$ | 0 | 0.0304 | 0.0255 | 0.0704 | 0.010 |
| UFF 0.2 | $E_{abs}$ | −178.584572 | −178.584220 | −178.582909 | −178.581144 | |
| | rms force | 0.000002 | 0.000006 | 0.000005 | 0.000004 | |
| | $E_{rel}$ | 0 | 0.0096 | 0.0452 | 0.0933 | 0.005 |
| UFF 0.1 | $E_{abs}$ | −178.584569 | −178.584264 | −178.582952 | −178.581187 | |
| | rms force | 0.000001 | 0.000010 | 0.000000 | 0.000000 | |
| | $E_{rel}$ | 0 | 0.0084 | 0.0440 | 0.0920 | 0.004 |
| Exp. | $G_{rel}$ | 0 | 0.0106 | 0.0480 | 0.0800 | |

to our demanding convergence, our results enable an accuracy discussion on the scale of the thousandth of eV, only the slight *b* uncertainty must be kept in mind.

### 2.4.2. Results

We now define the rms error as:

$$\mathrm{rms} = \frac{1}{3}\left[\sum_{i=b,c,d}\left(e_i^{\mathrm{calc}} - e_i^{\mathrm{exp}}\right)^2\right]^{1/2}, \quad \text{with } e_i^{\mathrm{calc}} = E_i^{\mathrm{calc}} - E_a^{\mathrm{calc}} \tag{5}$$

It can be seen in Table 4 that the rms errors are small: between 0.004 and 0.010 eV according to the method used. It can be seen that these values are largely dominated by the errors on *c* and *d*, this shows that the uncertainty on *b* (0.001 eV) has no consequence, and that the rms errors of Table 4 are significant.

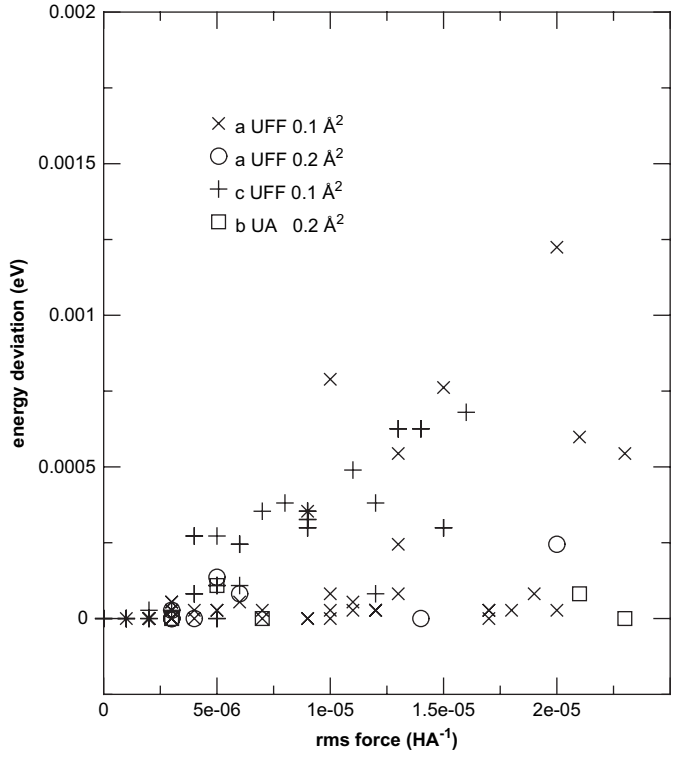


Figure 4. Graphical representation of the convergence behaviour of fully converged calculations: absolute value of the energy deviation towards residual rms force.

Since we have seen in Section 2.3 that thermal contributions only slightly affect the results, we may compare these results to experimental values. It can be seen that:

1. If the simple UA−UFF cavity is used the four conformers lie within 0.070 eV, which is close to the NMR value (0.080 eV). Nevertheless the *b*−*a* difference is obtained too large and *b* is even obtained less stable than *c*.
2. Using the UFF cavity yields excellent results, with only *d* a little too high.
3. If a finer tesselation of the surface is used (from 0.2 to 0.1 Å$^2$), then all the energy differences are reduced by only $\simeq$0.001 eV.

These results show that with the simple UA−UFF cavity the *b*−*c* energy difference has the wrong sign, and that providing the hydrogens with individual spheres restores the right sign. This success can be reasonably related to the specific steric hindrance in our molecule. It can be seen in Figure 2 that the naphthyl fragment is critically facing three H atoms of the isopropyl fragment (in *a* and *b*) and two H atoms of the dimethyl fragment (in *c* and *d*). Our results show that it is important to provide these H atoms with individual spheres.

## 2.5. Thermal contributions

Nuclear movements generally contribute to conformation energies because nuclear vibrations display ZPE (zero point energy) and because several vibration and rotation states may be accessible at the temperature of the experiment. Both these effects may differ in the various conformers. In this section all the energies are PCM energies, but we consider two possible origins of the vibration frequencies:

1. Harmonic frequencies are calculated in the vacuum, at the vacuum optimised geometry.

Table 5
Absolute (H) and relative (eV) free energies in $CDCl_3$: influence of the origin of the harmonic frequencies, PCM or in vacuum, rms error is in eV

| PCM cavity+av tess. area | | Harmonic analysis | *a* | *b* | *c* | *d* | rms error |
|---|---|---|---|---|---|---|---|
| UA − UFF 0.2 | $F_{abs}$ | UA−UFF 0.2 | −178.246697 | −178.245336 | −178.245851 | −178.244300 | |
| | | Vacuum | −178.245600 | −178.244393 | −178.244726 | −178.243369 | |
| | $F_{rel}$ | UA−UFF 0.2 | 0 | 0.0370 | 0.0230 | 0.0652 | 0.013 |
| | | Vacuum | 0 | 0.0328 | 0.0238 | 0.0607 | 0.013 |
| UFF 0.2 | $F_{abs}$ | UFF 0.2 | −178.237631 | −178.237292 | −178.236057 | −178.234528 | |
| | | Vacuum | −178.237877 | −178.237436 | −178.236279 | −178.234800 | |
| | $F_{rel}$ | UFF 0.2 | 0 | 0.0092 | 0.0428 | 0.0844 | 0.002 |
| | | Vacuum | 0 | 0.0120 | 0.0435 | 0.0837 | 0.002 |
| UFF 0.1 | $F_{abs}$ | UFF 0.1 | −178.237313 | −178.236986 | −178.235659 | −178.234264 | |
| | | Vacuum | −178.237514 | −178.237131 | −178.235971 | −178.234498 | |
| | $F_{rel}$ | UFF 0.1 | 0 | 0.0090 | 0.0450 | 0.0830 | 0.002 |
| | | Vacuum | 0 | 0.0105 | 0.0420 | 0.0821 | 0.002 |
| Exp. | $G_{rel}$ | | 0 | 0.0106 | 0.0480 | 0.0800 | |

2. They are calculated within the PCM method. Note that theoretical arguments actually make these PCM frequencies disputable.[37]

Results are given in Table 5. We have checked, like in Section 2.4, that the small values of the rms errors are significant, despite the small uncertainty on *b*. The results of Table 5 call for the following comments:

1. As expected from Section 2.3 thermal contributions never change the energetic order of the conformations. In particular the UA−UFF cavity still yields the wrong sign for the *b*−*c* energy difference.
2. The best results are obtained with the UFF cavity, this confirms that providing hydrogen atoms with individual spheres is more realistic.
3. If the UFF cavity is used, using a finer tesselation yields the same value of the rms error. This confirms that our tesselation has converged.
4. In all cases using PCM or vacuum frequencies yields the same rms error. Nevertheless note that with PCM frequencies the errors are more uniform (maximum error: 0.003 eV) than with vacuum frequencies (maximum error: 0.006 eV).
5. Comparison with Table 4 shows that thermal contributions, although small, actually do improve the results since the rms error is reduced by a factor two. This is mainly due to the *d* conformer.
6. The most striking result is the very small value of the UFF rms error: 0.002 eV (0.05 kcal/mol). This error has the same order of magnitude, though a little larger, as the error we have deduced from NMR errors (at most 0.0015 eV).

Since the present results are clearly consistent with the chemical shifts obtained in Section 2.2 we conclude that our interpretation of the NMR spectrum is valid. Our results show that the DFT and PCM methods yield free energies in excellent agreement with NMR measurements, under the condition that the sophisticated UFF cavity is used, with individual spheres on hydrogens.

### 2.6. Influence of the gaussian basis set

#### 2.6.1. Comparison with the 6-31+g(d) basis set

In the present work we have used the pSDD core pseudopotential and basis,[38] because of our experience of the general good performance of this basis. Since most of the calculations of the literature are done with basis sets of the Pople family[4] we have also used the 6-31+*g*(*d*) basis for the purpose of comparison. Results are given in Table 6.

It can be seen that the 6-31+*g*(*d*) residual forces are smaller than $10^{-5}$ and the rms error 0.006 eV. According to the

Table 6
Influence of the gaussian basis set: absolute (H) and relative values (eV) of the PCM energies (*E*) and free energies with vacuum frequencies (*F*) of the four conformers, residual rms forces (H Å$^{-1}$) and relative abundances at equilibrium at 210 K

| | Basis set | *a* | *b* | *c* | *d* | rms error |
|---|---|---|---|---|---|---|
| $E_{abs}$ | 6-31+*g*(*d*) | −1017.158959 | −1017.158303 | −1017.157176 | −1017.155257 | |
| $E_{rel}$ | — | 0 | 0.0179 | 0.0485 | 0.1007 | 0.007 |
| rms force | — | 0.000009 | 0.000005 | 0.000005 | 0.000000 | |
| $F_{abs}$ | — | −1016.813152 | −1016.812360 | −1016.811475 | −1016.809698 | |
| $F_{rel}$ | — | 0 | 0.0216 | 0.0456 | 0.0940 | 0.006 |
| $G_{rel}$ | Exp. | 0 | 0.0106 | 0.0480 | 0.0800 | |
| Abundance | 6-31+*g*(*d*) | 100 | 30.0 | 7.9 | 0.55 | |
| Abundance | pSDD | 100 | 51.1 | 9.0 | 0.98 | |
| Abundance | Exp. | 100 | 55.8 | 7.1 | 1.2 | |

uncertainty discussion of the previous sections, we think that this error value is significant. This value (0.006 eV) is significantly larger than that of our basis (0.002 eV). The largest errors display the same tendency: 0.014 eV for 6-31+$g(d)$ (conformer $d$) and 0.006 eV for pSDD (conformer $c$). The consequences of these errors are striking if abundances are considered: it can be seen in Table 6 that apart from conformer $c$, which is slightly better described by the Pople basis, 6-31+$g(d)$ abundances of conformers $b$ and $d$ are too small by a factor almost two.

### 2.6.2. Test of the Pople basis sets

In Table 7 we compare the conformation analysis in the vacuum yielded by several Pople type basis sets. Note that our pSDD basis has no $p$ gaussian on hydrogens and one $d$ gaussian on heavy atoms, with exponent 0.8 taken in the Pople basis: the comparison of Table 7 is fully significant, therefore. It can be seen that:

Table 7
Energy differences in the vacuum and rms errors (eV) for various basis sets

| Basis set | $a$ | $b$ | $c$ | $d$ | rms error |
|---|---|---|---|---|---|
| 6-31$g(d)$ | 0 | 0.0329 | 0.0883 | 0.1598 | 0.031 |
| 6-31+$g(d)$ | 0 | 0.0245 | 0.0847 | 0.1387 | 0.024 |
| 6-31++$g(d)$ | 0 | 0.0235 | 0.0847 | 0.1361 | 0.023 |
| 6-311$g(d)$ | 0 | 0.0307 | 0.0881 | 0.1519 | 0.028 |
| 6-311++$g(d)$ | 0 | 0.0237 | 0.0881 | 0.1371 | 0.024 |
| pSDD | 0 | 0.0181 | 0.0805 | 0.1340 | 0.021 |
| Exp. | 0 | 0.0106 | 0.0480 | 0.0800 | — |

1. The difference between the pSDD and 6-31+$g(d)$ rms errors is 0.003 eV, very close to the difference of the PCM values (0.004 eV). The present comparison of vacuum results is justified, therefore.
2. The 6-31$g(d)$ basis is very poor (rms error: 0.03 eV).
3. 6-31$g(d)$ and 6-311$g(d)$ are close to one another (0.03 eV), this shows that decontracting the basis is useless.
4. 6-31+$g(d)$, 6-31++$g(d)$ and 6-311++$g(d)$ results are close to one another (0.02 eV). This shows that adding diffuse gaussians is necessary, and that one shell is sufficient.

The 6-31+$g(d)$ is thus the best small basis of the Pople family. We emphasise that the pSDD basis is much smaller (373 gaussians) than the 6-31+$g(d)$ basis (479 gaussians). This difference is slightly perceptible as long as energies are calculated, but doubles the computation time of frequencies. Our basis is thus smaller and significantly better than the smallest diffuse Pople basis. We attribute this success to the core pseudopotentials, which enable a low cost, finer description of the valence zone. Also the Stuttgart–Dresden basis sets are free from the Pople constraint, of equal exponents for $s$ and $p$ primitives.

### 2.6.3. Structural test of a few basis sets: the formaldehyde case

The pSDD and 6-31+$g(d)$ structures of the four conformers also display slight differences, for instance the 6-31+$g(d)$ value of the vacuum CO distance (1.232 Å) is a little larger (by 0.007 Å) than the pSDD value (1.226 Å), and the 6-31+$g(d)$ values of the dipole moments are regularly 0.3 D smaller than the pSDD values.

Since exact values are not known for our molecule, we turn to formaldehyde, for which accurate values have been obtained, through inversion of rovibration data.[39] According to this work the CO bond length amounts to 1.2031 Å. We have calculated this formaldehyde value with several currently available basis sets: pSDD (1.2033 Å), 6-31+$g(d)$ (1.2093 Å), Dunning $D95V$ (1.2411 Å), and $aug{-}cc{-}pvtz$ (1.2002 Å). These results show that the pSDD value is in exceptional agreement with the accurate value. The CH bond length displays like tendencies, though less spectacular. If we now consider the dipole moment, with measured value 2.332 D,[34] we obtain pSDD (2.565 D), 6-31+$g(d)$ (2.515 D), $D95V$ (2.759 D) and $aug{-}cc{-}pvtz$ (2.389 D). It can be seen that pSDD and 6-31+$g(d)$ yield similar values, although slightly overestimated.

Of course the results depend on both the basis set and the functional. The present formaldehyde results suggest that the pSDD basis, coupled to the B3LYP functional, yields excellent molecular geometries. This can explain the success of this couple in conformational analysis.

## 3. Discussion

In this section we investigate two contributions, which are not always taken into account in the literature.

### 3.1. Non-electrostatic PCM contributions

In Table 8 we give the individual contributions of cavitation, Pauli repulsion and dispersion. It can be seen that if these contributions are neglected ($F^{el}_{pcm,rel}$ result), then the rms error amounts to 0.01 eV. Such a value has dramatic consequences on the conformer abundances. Table 8 shows that this effect can be attributed to cavitation energy for $a$ and $d$ and to dispersion energy for $c$.

Table 8
Different contributions to PCM energies: total and detailed non-electrostatic contributions (eV), cavity volume (Å$^3$), cavity surface (Å$^2$) and relative free energies (with vacuum harmonic analysis) without the PCM non-electrostatic contributions (eV)

| | $a$ | $b$ | $c$ | $d$ | rms error |
|---|---|---|---|---|---|
| $E^{non\ el}_{pcm}$ | 0.663 | 0.651 | 0.644 | 0.644 | |
| $E_{rep}$ | 0.047 | 0.046 | 0.048 | 0.046 | |
| $E_{disp}$ | −0.893 | −0.887 | −0.913 | −0.898 | |
| $E_{cav}$ | 1.510 | 1.492 | 1.509 | 1.495 | |
| Cavity volume | 414.80 | 414.29 | 406.04 | 407.73 | |
| Cavity surface | 328.94 | 327.60 | 330.96 | 327.89 | |
| $F^{el}_{pcm,rel}$ | 0 | 0.0239 | 0.0632 | 0.1031 | 0.010 |
| $G_{rel}$ exp. | 0 | 0.0106 | 0.0480 | 0.0800 | |

It is clear, intuitively, that solute–solvent dispersion is larger when the contact surface between them is larger. This feature is supported by the theory,[32,33] showing that the dispersion energy is an increasing function of the cavity surface. It

can be seen in Table 8 that *c* displays the larger value of the cavity surface.

Cavitation free energy is an increasing function of both cavity volume[30] and surface.[23] It can be seen in Table 8 that *b* and *d* display smaller values of both the cavity volume and surface than *a*. This feature contributes to the stabilisation of these conformers, relative to *a*. Note that *c*, displaying a smaller volume and a larger cavity surface than *a*, is attributed the same cavitation free energy.

In summary the PCM non-electrostatic terms yield a little, but significant, discrimination of the conformers. These terms can be rationalised in terms of molecular volume and surface. Neglect of these contributions deteriorates the conformation analysis.

### 3.2. Thermal effects

It has been shown in Section 2.5 that thermal vibrational contributions have a slight but positive effect, dropping the rms error from 0.004 to 0.002 eV. We have investigated the following issues:

1. Since harmonic analysis is doubtfull for low frequency modes we have dropped the six smallest modes, with a frequency smaller than 100 $cm^{-1}$, from the harmonic analysis. This procedure does modify the absolute free energies, but leaves the final rms error unaffected.
2. We have also checked that using scaling factors, as published for the B3LYP functional and the 6-31*g*(*d*) basis set (0.9989 for the vibration enthalpy and 1.0015 for the vibration entropy)[40] does no affect the results.
3. We have found out that thermal analysis can be done indifferently at the real temperature, 210 K or at 0 K. This means that the improvement yielded by thermal analysis is only due to vibrational ZPEs. Actual values of the ZPEs: 0.3660 H (conformers *a*, *b* and *c*) and 0.3658 H (conformer *d*) show that *d* is slightly floppier than the other conformers.

As is well known harmonic analysis should always be done, at least for minima characterisation. Our results show that it also enables a better description of the *d* conformer.

## 4. Conclusion

The *S*-3-(1-naphthoyl)-4-isopropyl-2,2-dimethyloxazolidin-5-one displays four conformers, *a* (*P* cis), *b* (*M* cis), *c* (*P* trans) and *d* (*M* trans). The low temperature NMR spectrum in $CDCl_3$ shows that these conformers lie within 0.08 eV at 210 K. Since GIAO calculations of the chemical shifts only yield a plausible interpretation of the spectrum, validation of this interpretation requires an accurate conformation analysis. We have obtained values of the free energies, which are fully consistent with NMR data and with calculated chemical shifts with the following protocol:

1. We use the UFF cavity, with spheres on every atom, including hydrogens. Tesselation with 0.1 or 0.2 $Å^2$ average area is sufficient.
2. We calculate energies with the B3LYP functional and the Stuttgart–Dresden core pseudopotentials and polarised basis set.
3. We ensure a demanding convergence of the DFT calculations with all residual forces smaller than $10^{-5}$ H $Å^{-1}$.
4. We take non-electrostatic PCM contributions and thermal contributions into account.

Within this protocol our rms error amounts to 0.002 eV (0.05 kcal/mol), which is very small for a 44 atom molecule in solution, and close to the experimental uncertainty. Deviation from this protocol: use of Pople basis sets, use of united-atom cavities, neglect of non-electrostatic terms and of thermal contributions, lack of convergence of the DFT calculations, can yield significant errors and even change the signs of the energy differences.

## 5. Technical details

### 5.1. Computations

All the quantum calculations have been done with the DFT method and the B3LYP functional,[41] integrated on a very fine grid including 99 radial shells and 590 angular points per shell on each atom.[42] All geometry optimisations have been performed with the 'Stuttgart–Dresden' core pseudopotentials and gaussian basis set (SDD),[38] supplemented with polarisation *d* gaussians on C, N and O atoms (exponent 0.8, taken from Ref. 4). This polarised SDD basis is referred to as pSDD. Core pseudopotentials are an efficient tool for reducing computation times: all the core electrons, in the present case all 1s electrons of C, N and O atoms are dropped from the calculation and their influence simulated by additional terms in the hamiltonian operator.

Since NMR chemical shifts bear witness of the electron density close to nuclei, the use of core pseudopotentials is in principle precluded. For this reason we have calculated the chemical shifts with the 6-31*g*(*d*,*p*) and 6-311+*g*(2*d*,*p*) Pople basis sets[4] at the geometries optimised with the pSDD basis.

The Gaussian 03, Rev C02 package[42] has been used throughout this work and found efficient if some care is taken. In particular, geometry optimisations and frequency calculations in solution have always been done in two separate steps.

Since inaccuracy of the energies has dramatic consequences on the conformer abundances, we here specify the conversion factors between Hartree, eV and Kelvin that we have used: 1 H=27.211411 eV and 1 H=11604.903524 K. These values come from recent values of the fundamental constants, taken from Ref. 43.

### 5.2. Materials

Reaction was conducted in oven dried glassware under an atmosphere of dry argon gas. Acetone was purchased with water <50 ppm. High temperature $^1H$ NMR spectra were measured at 360 MHz using DMF-$d_7$ as solvent. Chemical shifts are reported in units to 0.01 ppm precision with coupling

constants reported to 0.1 Hz precision using internal dimethylformamide ($\delta$ 8.03, 2.92, 2.75 ppm) as an internal reference. Multiplicities are reported as follows: s=singlet, d=doublet, t=triplet, q=quartet, m=multiplet, br s=broad singlet. $^{13}C$ NMR spectra were measured at 90 MHz on a Bruker AC360 using DMF ($\delta$ 163.15, 34.89, 29.76 ppm) as an internal reference. Infrared spectra were recorded as thin film on NaCl plates using a Perkin–Elmer Spectrum One FTIR spectrophotometer. Mass spectra were measured on MAT 95S Finnigan-Thermo spectrometer at the Institut de Chimie Moléculaire d'Orsay (ICMMO) Mass Spectrometry Laboratory. Elemental analysis has been performed at the ICSN 91198 Gif sur Yvette Cedex, France.

To a stirred suspension of sodium L-valinate (2.00 g, 14.38 mmol) and oven dried 4 Å molecular sieves in extra-dry acetone (40 mL) at 0 °C under argon atmosphere is slowly added boron trifluoride etherate (100 mL, 0.82 mmol). The mixture is stirred 5 min at 0 °C and 15 h at room temperature. Then, 1-naphthoyl chloride (2.16 mL, 14.38 mmol) is added and the reaction mixture is stirred for 2 h. The final mixture is filtered through Celite and molecular sieves are washed with ether (2×20 mL). Solvents are evaporated and the resulting solid is dried under high vacuum for 1 h. After dilution in ether (60 mL) the organic layer is washed with a saturated sodium hydrogenocarbonate solution (30 mL) and water (30 mL). Solvents are evaporated to give the crude oxazolidinone **2** (3.91 g). Purification by flash chromatography (pentane/ether 80:20) affords pure oxazolidinone **2** (3.28 g, 73%, ee>99%) as a white powder.

$R_f$=0.32 (pentane/ether 7:3); white crystals, mp=112 °C; $[a]_D^{20}$ +178 (*c* 1.00, $CH_2Cl_2$); $^1H$ NMR (360 MHz, 373 K, $(CD_3)_2NCOD$) $\delta$ 0.67 (d, *J*=7.0 Hz, 3H), 0.81 (d, *J*=7.0 Hz, 3H), 1.47 (m, 1H), 1.92 (s, 3H), 1.96 (s, 3H), 4.57 (br s, 1H), 7.55–7.66 (m, 3H), 7.78–7.84 (m, 1H), 7.92–7.97 (m, 1H), 7.99–8.10 (m, 2H); $^{13}C$ NMR (90 MHz, 353 K, $(CD_3)_2NCOD$) $\delta$ 15.9, 17.8, 26.0, 26.7, 30.6, 62.8, 97.2, 124.3, 124.8, 125.2, 126.7, 127.4, 128.8, 130.0, 130.1, 133.8, 134.3, 167.7, 169.2; IR (thin film): 1785, 1651, 1646, 1409, 1379, 1339, 1258, 784 $cm^{-1}$; LRMS (ES): 334.1 $[M+Na]^+$, 645.3 $[2M+Na]^+$ *m/z*; HRMS (ES): $[M+Na]^+$ calculated 334.1414, found 334.1416. Elemental analysis calcd (%) for $C_{19}H_{21}NO_3$ (311.4): C 73.29, H 6.80, N 4.50; found: C 73.34, H 6.94, N 4.61.

### 5.3. Spectral measurements

Low temperature $^1H$ NMR spectra were measured at 400 MHz on a Bruker Avance DRX 400 using $CDCl_3$ as solvent. Chemical shifts are reported in $\delta$ units using residual chloroform ($\delta$ 7.27 ppm) as an internal reference. Low temperature calibration was done with methanol at low temperature.[44]

## Acknowledgements

We thank the Ministère de la Recherche et de l'Éducation for a grant (M.B.), the CNRS (UMR 8182) and the Université Paris-Sud for financial support. We thank Jean-Pierre Baltaze (ICMMO, UMR 8182) for helping us with NMR at low temperature.

## References and notes

1. Lam, P. C. H.; Carlier, P. *J. Org. Chem.* **2005**, *70*, 1530.
2. Paisz, B.; Simonyi, M. *Chirality* **1999**, *11*, 651.
3. Nandini, G.; Sathyanarayana, D. N. *J. Mol. Struct. Theochem.* **2003**, *638*, 4730.
4. Hariharan, P. C.; Pople, J. A. *Theor. Chim. Acta* **1973**, *28*, 213.
5. Bowles, P.; Clayden, J.; Helliwell, M.; Mac Carthy, C.; Tomkinson, M.; Westlund, N. *J. Chem. Soc., Perkin Trans. 1* **1997**, 2607.
6. Bragg, R. A.; Clayden, J.; Morris, G. A.; Pink, J. H. *Chem.—Eur. J.* **2002**, *8*, 1279.
7. Ahmed, A.; Bragg, R. A.; Clayden, J.; Lai, L. W.; Mac Carthy, C.; Pink, J. H.; Westlund, N.; Yasin, S. A. *Tetrahedron* **1998**, *54*, 13277.
8. Clayden, J. *Ang. Chem., Int. Ed.* **1997**, *36*, 949.
9. Clayden, J.; Vassiliou, N. *Org. Biomol. Chem.* **2006**, *4*, 2667.
10. Clayden, J.; Lund, A.; Vallverdu, L.; Helliwell, M. *Nature (London)* **2004**, *431*, 966.
11. Clayden, J. *Chem. Commun.* **2004**, 127.
12. Clayden, J. *Synlett* **1998**, 810.
13. Clayden, J.; Lund, A.; Youssef, L. H. *Org. Lett.* **2001**, *3*, 4133.
14. Zhang, Y.; Wang, Y.; Dai, W. M. *J. Org. Chem.* **2006**, *71*, 2445.
15. Dai, W. M.; Yeung, K. K. Y.; Liu, J. T.; Zhang, Y.; Williams, I. D. *Org. Lett.* **2002**, *4*, 1615.
16. Dai, W. M.; Yeung, K. K. Y.; Wang, Y. *Tetrahedron* **2004**, *60*, 4425.
17. Dai, W. M.; Yeung, K. K. Y.; Chow, C. W.; Williams, I. D. *Tetrahedron: Asymmetry* **2001**, *12*, 1603.
18. Tomasi, J.; Persico, M. *Chem. Rev.* **1994**, *94*, 2027.
19. Cramer, C. J.; Truhlar, D. J. *Chem. Rev.* **1999**, *99*, 2161.
20. Tomasi, J.; Cami, R.; Menucci, B.; Cappelli, C.; Corni, S. *Phys. Chem. Chem. Phys.* **2002**, *4*, 5697.
21. Pascual Ahuir, J. L.; Silla, E. *J. Comput. Chem.* **1990**, *11*, 1047.
22. Rappé, A. K.; Casewit, C. J.; Colwell, K. S.; Goddard, W. A., III; Skiff, W. M. *J. Am. Chem. Soc.* **1992**, *114*, 10024.
23. Barone, V.; Cossi, M.; Tomasi, J. *J. Chem. Phys.* **1997**, *107*, 3210.
24. Mac Quarrie, D. *Statistical Mechanics*; Harper & Row: New York, NY, 1976.
25. Ben-Naim, A.; Marcus, Y. *J. Chem. Phys.* **1984**, *81*, 2016.
26. Wolinski, K.; Hilton, J. F.; Pulay, P. *J. Am. Chem. Soc.* **1990**, *112*, 8251.
27. Abraham, R. J.; Bardsley, B.; Mobli, M.; Smith, R. J. *Magn. Reson. Chem.* **2005**, *43*, 3.
28. Colombo, D.; Ferraboschi, P.; Ronchetti, F.; Toma, L. *Magn. Reson. Chem.* **2002**, *40*, 581.
29. Reed, A. E.; Weinstock, R. B.; Weinhold, F. *J. Chem. Phys.* **1985**, *83*, 735.
30. Pierotti, R. A. *Chem. Rev.* **1976**, *76*, 717.
31. Huron, M. J.; Claverie, P. *J. Phys. Chem.* **1972**, *76*, 2123.
32. Floris, F.; Tomasi, J. *J. Comput. Chem.* **1989**, *10*, 616.
33. Floris, F.; Tomasi, J.; Pascual Ahuir, J. L. *J. Comput. Chem.* **1991**, *12*, 784.
34. *Handbook of Chemistry and Physics*; CRC: London, 1995.
35. Peng, C.; Ayala, P. Y.; Schlegel, H. B.; Frisch, M. J. *J. Comput. Chem.* **1996**, *17*, 49.
36. Farkas, O.; Schlegel, H. B. *Chem. Rev.* **1999**, *111*, 10806.
37. Klamt A. Communication to the Computational Chemistry List, http://www.ccl.net/htdig.
38. Fuentealba, P.; Preuss, H.; Stoll, H.; Szentpaly, L. v. *Chem. Phys. Lett.* **1989**, *89*, 418.
39. Carter, S.; Handy, N. *J. Mol. Spectrosc.* **1996**, *179*, 65.
40. Scott, A. P.; Radom, L. *J. Phys. Chem.* **1996**, *100*, 16502.
41. Becke, A. D. *J. Chem. Phys.* **1993**, *98*, 5648.
42. Frisch, M. J.; Trucks, G. W.; Schlegel, H. B.; Scuseria, G. E.; Robb, M. A.; Cheeseman, J. R.; Montgomery, J. A., Jr.; Vreven, T.; Kudin, K. N.; Burant, J. C.; Millam, J. M.; Iyengar, S. S.; Tomasi, J.; Barone, V.; Mennucci, B.; Cossi, M.; Scalmani, G.; Rega, N.; Petersson, G. A.; Nakatsuji, H.; Hada, M.; Ehara, M.; Toyota, K.; Fukuda, R.; Hasegawa, J.; Ishida, M.; Nakajima, T.; Honda, Y.; Kitao, O.; Nakai, H.; Klene,

M.; Li, X.; Knox, J. E.; Hratchian, H. P.; Cross, J. B.; Adamo, C.; Jaramillo, J.; Gomperts, R.; Stratmann, R. E.; Yazyev, O.; Austin, A. J.; Cammi, R.; Pomelli, C.; Ochterski, J. W.; Ayala, P. Y.; Morokuma, K.; Voth, G. A.; Salvador, P.; Dannenberg, J. J.; Zakrzewski, V. G.; Dapprich, S.; Daniels, A. D.; Strain, M. C.; Farkas, O.; Malick, D. K.; Rabuck, A. D.; Raghavachari, K.; Foresman, J. B.; Ortiz, J. V.; Cui, Q.; Baboul, A. G.; Clifford, S.; Cioslowski, J.; Stefanov, B. B.; Liu, G.; Liashenko, A.; Piskorz, P.; Komaromi, I.; Martin, R. L.; Fox, D. J.; Keith, T.; Al-Laham, M. A.; Peng, C. Y.; Nanayakkara, A.; Challacombe, M.; Gill, P. M. W.; Johnson, B.; Chen, W.; Wong, M. W.; Gonzalez, C.; Pople, J. A. *Gaussian 03, Revision C.02*; Gaussian: Wallingford, CT, 2004.

43. Cohen, E. R.; Taylor, B. N. *The 1986 Adjustment of the Fundamental Physical Constants*. CODATA Bulletin; Pergamon: Elmsford, NY, 1986.
44. Berger, S.; Braun, S. *200 and More NMR Experiments: A Practical Course*; Wiley: Weinheim, 2004; p 141.